Molecular Neurobiology (2019) 56:2524–2541
https://doi.org/10.1007/s12035-018-1244-0

Anionic Phospholipids Bind to and Modulate the Activity of Human TRESK Background K^+ Channel

Jonathan P. Giblin[1,2] · Iñigo Etayo[1] · Aida Castellanos[1,2] · Alba Andres-Bilbe[1,2] · Xavier Gasull[1,2]

Received: 18 April 2018 / Accepted: 15 July 2018 / Published online: 23 July 2018

Abstract

The background K^+ channel TRESK regulates sensory neuron excitability, and changes in its function/expression contribute to neuronal hyperexcitability after injury/inflammation, making it an attractive therapeutic target for pain-related disorders. Factors that change lipid bilayer composition/properties (including volatile anesthetics, chloroform, chlorpromazine, shear stress, and cell swelling/shrinkage) modify TRESK current, but despite the importance of anionic phospholipids (e.g., PIP_2) in the regulation of many ion channels, it remains unknown if membrane lipids affect TRESK function. We describe that both human and rat TRESK contain potential anionic phospholipid binding sites (apbs) in the large cytoplasmic loop, but only the human channel is able to bind to multilamellar vesicles (MLVs), enriched with anionic phospholipids, suggesting an electrostatically mediated interaction. We mapped the apbs to a short stretch of 14 amino acids in the loop, located at the membrane-cytosol interface. Disruption of electrostatic lipid-TRESK interactions inhibited hTRESK currents, while subsequent application of Folch Fraction MLVs or a PIP_2 analog activated hTRESK, an effect that was absent in the rat ortholog. Strikingly, channel activation by anionic phospholipids was conferred to rTRESK by replacing the equivalent rat sequence with the human apbs. Finally, in the presence of a calcineurin inhibitor, stimulation of a $G_{q/11}$-linked GPCR reduced hTRESK current, revealing a likely inhibitory effect of membrane lipid hydrolysis on hTRESK activity. This novel regulation of hTRESK by anionic phospholipids is a characteristic of the human channel that is not present in rodent orthologs. This must be considered when extrapolating results from animal models and may open the door to the development of novel channel modulators as analgesics.

Keywords K2P channels · KCNK · Membrane phospholipids · Nociception · Neuronal excitability

Introduction

TWIK-related spinal cord K^+ channel (TRESK) or $K_{2P}18.1$ (encoded by the *KCNK18* gene) is a member of the two-pore domain potassium channel (K_{2P}) family, which contains 15 members with a shared molecular architecture. K_{2P} channel proteins are comprised of four transmembrane domains and two pore-loop forming domains with intracellular N- and C-termini [1]. Four pore-loops are required to form a functional K^+ selectivity filter and therefore K_{2P} channels function as dimers, unlike the other K^+ channel subfamilies (voltage-gated, calcium-activated, and inwardly rectifying K^+ channels), which function as tetramers [2, 3]. K_{2P} channels play an important role in the maintenance and stabilization of the resting membrane potential, and in excitable cells such as neurons and cardiac myocytes, they modulate the shape and frequency of action potentials. They have been implicated in a wide range of physiological processes including nociception, somatosensation, nutrient and chemo-sensing, hormone secretion, sleep, and anesthesia [4–7].

The coding sequence of the human *KCNK18* gene was originally identified by a homology search of the draft human genome using the amino acid sequence of a previously identified K_{2P} channel, $K_{2P}1.1$ (also known as TWIK1, tandem of pore domains in a weak inwardly rectifying K^+ channel), which led to its cloning from human spinal cord mRNA [8]. TRESK is selectively expressed in a subpopulation of sensory neurons of the dorsal root (DRG) and trigeminal ganglia (TG), which

Electronic supplementary material The online version of this article (https://doi.org/10.1007/s12035-018-1244-0) contains supplementary material, which is available to authorized users.

✉ Xavier Gasull
xgasull@ub.edu

[1] Neurophysiology Lab, Department of Biomedicine, Medical School, Institute of Neurosciences, Universitat de Barcelona, Casanova 143, 08036 Barcelona, Spain

[2] Institut d'Investigacions Biomèdiques August Pi i Sunyer (IDIBAPS), 08036 Barcelona, Spain

innervate peripheral regions of the body and are responsible for the detection of both innocuous (e.g., touch) and noxious chemical, thermal, and mechanical stimuli [9–14]. Studies on primary cultures demonstrated that TRESK accounts for a significant proportion of the "resting" or background K^+ conductance in DRG neurons from mouse and rat [11, 15]. The first evidence of a role for TRESK in the regulation of sensory neuron excitability came when DRG neurons from a mutagenized mouse strain carrying a loss-of-function mutation in the *Kcnk18* gene were compared with wild-type DRG neurons, revealing that the TRESK-mutant neurons were easier to excite by depolarizing stimuli [11]. Subsequent studies have demonstrated that pharmacological inhibition of TRESK by alkylamides, such as hydroxy-α-sanshool and isobutylalkylamide (IBA) or pyrethroids, produces sensory neuron activation and contributes to associated somatosensory and nocifensive behaviors [9, 10, 16, 17]. A dominant negative loss-of-function mutation in the *KCNK18* gene is linked to familial migraine with aura, and over-expression of mouse TRESK with the equivalent mutation in trigeminal neurons was shown to cause hyperexcitability, suggesting that TRESK is required for correct regulation of trigeminal neuron excitability [18, 19]. An alteration of TRESK functional expression may also be a contributing factor to the changes in sensory neuron excitability observed during inflammation and neuropathic pain since *Kcnk18* mRNA and protein expression are decreased in rat models of neuropathic pain [10, 20] and TRESK activity is inhibited in the presence of inflammatory mediators such as arachidonic acid [8, 21]. Increased TRESK activity as a consequence of over-expression was shown to dampen the excitability of TG and DRG neurons and could attenuate nerve-injury-induced allodynia, leading to the suggestion that augmenting TRESK activity may be a viable therapeutic strategy for the treatment of pain-related conditions [20, 22–24]. A better understanding of the underlying mechanisms that influence TRESK activity is essential for the rational design of novel channel modulators.

The activity of TRESK can be modulated by stimuli that produce changes in the composition and/or properties of the plasma membrane. In a recent study from our laboratory, we demonstrated that TRESK activity can be modulated by experimentally applied shear stress, changes in osmotic pressure, and by compounds that affect membrane bilayer properties, such as chloroform and chlorpromazine [21]. Volatile (e.g., isofluorane) and local (e.g., bupivacaine) anesthetics are potent enhancers and inhibitors of TRESK currents, respectively [25]. Although the precise molecular mechanisms of action are unclear, volatile anesthetics appear to modify ion channel activity via their incorporation into lipid bilayers and by binding to amphiphilic sites on channel proteins [26].

TRESK currents are strongly potentiated by increases in intracellular Ca^{2+}-concentration via Ca^{2+}-dependent binding of the activated phosphatase calcineurin to the channel, which mediates dephosphorylation of inhibitory phosphorylation sites [27, 28]. This mechanism underlies the enhancement of TRESK activity observed upon $G_{q/11}$-coupled receptor stimulation [27, 29, 30]. However, G_q-coupled receptor activation can also produce large decreases in the plasma membrane concentration of the phosphoinositide phosphatidyl-inositol-4,5-bisphosphate (PIP_2) via the stimulation of phospholipase C (PLC) activity, which hydrolyses PIP_2 to produce diacylglycerol (DAG) and IP_3 [31–33]. It is also of note that large influxes of Ca^{2+} via TRP channels that co-express with TRESK in sensory neurons have also been shown to have significant effects on global PIP_2 levels via activation of Ca^{2+}-activated PLC isoforms, for example, the PLCδs, which are expressed in sensory neurons [34, 35]. Given the importance of PIP_2 in the regulation of the activity of a wide variety of ion channels and transporters [36] and the evidence for the role of PIP_2 in the regulation of other K_{2P} channels [37–39], it is feasible that changes in plasma membrane PIP_2 concentration may also contribute to physiological modulation of TRESK activity.

It is clear that the membrane environment and changes in lipid composition play an important role in the modulation of TRESK. However, there is no information to date regarding interactions between TRESK and membrane phospholipids and the consequences for channel function. In this study, we have investigated whether TRESK contains binding sites for membrane phospholipids and whether these interactions play a role in the modulation of channel activity.

Materials and Methods

In Silico Search for Putative Anionic Phospholipid Binding Sites

The primary sequences of human (GenBank accession number NP_862823.1) and rat (GenBank accession number AAS68516.1) TRESK were analyzed using the BH search program (available at http://helixweb.nih.gov/bhsearch). The threshold BH value for residues forming part of a potential membrane binding site was 0.6, and the search was performed with a window size of 10 to obtain scores for N- and C-terminal residues [40]. A search for the most common putative lipid-binding domains (the PH, PKC C1, PKC C2, PX, FYVE, GLA, GRAM, F-BAR, and ENTH domains) in human and rat TRESK was undertaken using the SMART program [41, 42].

Molecular Biology

Rat TRESK in the pcDNA3.1(+) vector (kindly provided by Dr. S. Yost, University of California-San Francisco, USA) was subcloned into the pEGFP-C3 vector (Clontech) using a *BamHI/XbaI* digest and used for transient transfection of cell

lines as previously described [21]. Human TRESK pcDNA3.1(+) vector was kindly provided by Dr. Y. Sano (Astellas Pharma Inc., Ibaraki, Japan) and subcloned into pEGFP-C2 (Clontech) vector with an *EcoRI/SmaI* digest [21]. pEGFP-mTREK-1 was a kind gift from Dr. G. Sandoz (CNRS-Universite de Nice-Sophia Antipolis, France). pRK5-HA-mGluR5 vector was kindly provided by Dr. F. Ciruela (University of Barcelona, Spain). pNice-CiVSP was kindly provided by Dr. S.C. Kohout (Montana State University, MT, USA). hTRPA1-GFP was a kind gift from Dr. F. Viana (Instituto de Neurociencias-CSIC, Alicante, Spain).

GST-Fusion Proteins PCR fragments of the relevant portions of human or rat TRESK were produced, with addition of a 5′ *BamHI* and 3′ *XhoI* sites using primer 5′ overhangs before subcloning into the pGEX-5X-3 vector (GE Healthcare) with a *BamHI/XhoI* digest. The in-frame stop codon present in the pGEX-5X-3 polylinker was used in all fusion proteins except for GST-hTRESK$_{(356–384)}$, where a stop codon was added on the 5′ overhang of the reverse primer. The sequences of the oligonucleotide primers used to generate each fusion protein are provided in supplementary methods.

Human-Rat TRESK Chimeras Human-rat TRESK chimeras were constructed using a splicing by overlap extension PCR strategy. A vertebrate Kozak sequence was added to the 5′ overhang of the forward flanking primer (GCCGCCACC) before the start codon to optimize protein expression of the chimeric constructs. For hTRESK$_{(1–163)}$-rTRESK$_{(185–405)}$ (hTRESK-rat-loop-rTRESK) and rTRESK$_{hTRESK(163–177)}$ (rTRESK-h-apbs), spliced PCR products were subcloned into pcDNA3.1(+) (ThermoFisher Scientific) with *BamHI/EcoRI* digests. The rTRESK$_{(1–184)}$-hTRESK$_{(163–384)}$ (rTRESK-human-loop-hTRESK) and hTRESK$_{rTRESK(184–197)}$ (hTRESK-r-apbs) constructs were subcloned into pcDNA3.1(+) with *BamHI/XhoI* digests. All restriction enzyme sites were added using primer 5′ overhangs. The sequences of the oligonucleotide primers used to generate each chimera are provided in supplementary methods.

Purification of GST Fusion Proteins

Growth of Bacterial Cultures Plasmids encoding the relevant fusion proteins were transformed into *Escherichia coli* (strain BL21, Novagen). Cultures were grown at 37 °C in minimal medium (0.4% (*w*/*v*) glucose, 1% (*w*/*v*) tryptone) supplemented with M9 salts (48 mM Na_2HPO_4, 22 mM KH_2PO_4, 8.6 mM NaCl, 18.7 mM NH_4Cl), 2 mM $MgSO_4$, 0.1 mM $CaCl_2$, and 100 mg/ml ampicillin until the OD_{600} reached 0.5–0.7. After reaching the desired OD_{600}, expression of the fusion proteins was induced by addition of isopropyl-β-D-1-thiogalactopyranoside (IPTG) to a final concentration of 0.1 mM followed by incubation at 25 °C for 3 h. Note that GST alone was induced with 1 mM IPTG. Bacteria were harvested by centrifugation at 3000*g* for 30 min at 4 °C, and pellets were stored at − 20 °C until use in the purification procedure.

Purification Procedure Frozen pellets were resuspended in purification buffer supplemented with a protease inhibitor cocktail (phosphate-buffered saline [containing $CaCl_2$ and $MgCl_2$, Sigma-Aldrich, Spain], 0.5% (*v*/*v*) Tween-20, 0.5 mM EDTA, 0.5 mM PMSF, 1 μg/ml Aprotinin, 1 μg/ml Pepstatin, 1 μg/ml Leupeptin, and 1 μg/ml Antipain). Bacteria were subsequently lysed using a probe sonicator, and insoluble material was removed by centrifugation at 20,000*g* for 30 min at 4 °C. The supernatant was applied to a column containing Glutathione Sepharose (GE Healthcare, Spain), which had been pre-equilibrated with purification buffer, and allowed to flow through under gravity. The column was washed three times with 10 column volumes of purification buffer followed by two washes with 10 column volumes of purification buffer (without Tween-20). After washing, fusion proteins were eluted with 50 mM TrisHCl, pH 8 containing 10 mM glutathione. Glycerol was subsequently added to a final concentration of 10% (*v*/*v*), and proteins were stored at − 20 °C until use in liposome binding assays.

Preparation of Liposomes for Liposome Binding Assay

Preparation of Folch Multilamellar Vesicles (MLVs) MLVs composed of Folch fraction I lipids were prepared from a 100 mg/ml stock solution in chloroform obtained from Sigma-Aldrich (Spain; Ref. B1502). Chloroform from an aliquot of stock lipids was evaporated under a stream of nitrogen gas and the residue further dried under a vacuum for 1 h (SpeedVac). Dried lipids were then resuspended in liposome binding buffer (20 mM HEPES KOH pH 7.4, 100 mM KCl, 1 mM EDTA) at a concentration of 1 mg/ml and incubated at 37 °C for 1 h with occasional vortexing. The resuspended lipids were stored at 4 °C and used within 24 h in the liposome-binding assay.

Preparation of MLVs of Defined Phospholipid Composition MLVs of defined phospholipid composition were prepared at a final concentration of 1 mM by mixing together different molar percentages of chloroform stock solutions of 1,2-dioleoyl-*sn*-glycero-3-phosphocholine (PC, Catalogue number 850375P, Avanti Polar Lipids, Alabama, USA), 1,2-dioleoyl-*sn*-glycero-[phospho-L-serine] (PS, Catalogue number 840035P, Avanti Polar Lipids), and 1,2-dioleoyl-*sn*-glycero-3-[phosphoinositol-4,5-bisphosphate] (PIP_2, Catalogue number 850155P, Avanti Polar Lipids) as indicated in the text and figure legends. Dried lipids were then rehydrated by treatment in the same manner as the Folch fraction lipids.

Liposome Binding Assay All steps were performed at room temperature. Five micrograms of purified GST fusion protein was incubated with 100 μg liposomes in a total volume of 150 μl for 30 min followed by centrifugation at 21,000*g* for 1 h. After centrifugation, the supernatant was removed and 150 μl 2× Laemmli loading buffer (250 mM Tris HCl pH 6.8, 40% (*v*/*v*) glycerol, 8% (*w*/*v*) SDS, 0.008% Bromophenol blue, 20% (*v*/*v*) β-mercaptoethanol) was added. The pellet was resuspended in 150 μl liposome binding buffer followed by addition of 150μl 2× Laemmli loading buffer. Samples were incubated at 95 °C for 3 min before equivalent amounts of supernatant and pellet were analyzed by SDS-PAGE followed by Coomassie staining.

HEK293 Cell Line Culture and Transfection

HEK293T cells were cultured in DMEM with 10% FBS, 1% penicillin/streptomycin, and 1% glutamine, maintained at 37 °C and 5% CO_2 and seeded in 12-mm dishes 24 h before transfection. Cells were transiently transfected with EGFP-hTRESK, EGFP-rTRESK, and EGFP-mTREK-1 vectors, or cotransfected with pRK5-HA-mGluR5, hTRPA1-GFP or pNice-CiVSP, and EGFP-hTRESK vectors using X-tremeGENE 9 transfection reagent (Roche, Mannheim, Germany), according to the manufacturer's instructions. Cells were used for patch-clamp experiments 24–48 h after transfection.

Electrophysiological Recordings

Electrophysiological recordings were performed as previously described [17, 43]. Briefly, recordings were performed with a patch-clamp amplifier (Axopatch 200B, Molecular Devices, Union City, CA) in transfected HEK293T cells. Patch electrodes were fabricated in a Flaming/Brown micropipette puller P-97 (Sutter instruments, Novato, CA). Membrane currents were recorded in excised patches of membrane using the inside-out configuration of the patch clamp technique, filtered at 2 kHz, digitized at 10 kHz, and acquired with pClamp 10 software. Electrodes had a resistance between 2 and 4 MΩ when filled with extracellular solution (in mM) 145 NaCl, 5 KCl, 2 $CaCl_2$, 2 $MgCl_2$, 10 HEPES, and 5 glucose at pH 7.4; and bath solution (in mM) 140 KCl, 2.1 $CaCl_2$, 2.5 $MgCl_2$, 5 EGTA, 10 HEPES, and 2 ATP at pH 7.3. In these conditions, the K^+ gradient across the patch is equivalent to that found in physiological conditions. One second depolarizing ramps from − 100 to + 100 mV every 10 s were used to record TRESK- or TREK-1-mediated currents. A holding voltage of − 80 mV was used. In whole-cell experiments, which were used to study the effect of mGluR5 activation on hTRESK current, the pipette solution was (in mM) 155 KCl, 5 EGTA, 3$MgCl_2$, and 10 HEPES. FK-506 (1 μM; Sigma-Aldrich, Madrid) was included in the pipette to block calcineurin activity. The same extracellular solution (bath) was used. In cell-attached experiments in cells cotransfected with mGluR5 and hTRESK, the pipette contained the extracellular solution used in the bath. Data was analyzed with Clampfit 10 (Molecular Devices) and Prism 5 (GraphPad Software, Inc., La Jolla, CA). Series resistance was always kept below 15 MΩ and compensated at 70–80%. All recordings were done at room temperature (22–23 °C), 24–48 h after transfection.

Statistical Analysis

Data are presented as mean ± SEM. Statistical differences between different sets of data were assessed by performing paired or unpaired Student's *t* test as indicated. Statistical significance was set at $*p < 0.05$; $**p < 0.01$; $***p < 0.001$.

Results

Identification of Putative Binding Sites for Anionic Phospholipids in TRESK Using an In Silico Approach

In general, protein regions that associate with biological membranes do so via binding to anionic/acidic phospholipids, displaying a wide variation in binding mechanisms [44]. In initial studies, we used an in silico approach to search for putative lipid-binding domains in both the human and rat isoforms of TRESK. A search for the most common putative lipid-binding domains (the PH, PKC C1, PKC C2, PX, FYVE, GLA, GRAM, F-BAR, and ENTH domains) in TRESK using the SMART program [41, 42] yielded no positive results, indicating that it is unlikely that TRESK contains lipid-binding domains with a well-defined tertiary structure. However, there are numerous examples of K^+ channels lacking these structurally defined lipid-binding domains that can still bind to acidic/anionic phospholipids via clusters of basic and hydrophobic amino acids [37, 45–48]. With this in mind, we analyzed the sequences of human and rat TRESK using BH search, a program that identifies putative membrane-binding sites on the basis of basic and hydrophobic amino acid content (available at http://helixweb.nih.gov/bhsearch) [40]. The results of this analysis are shown in Fig. 1. It identified two putative membrane-binding sites in human TRESK, one in the large cytoplasmic loop at the membrane-cytosol interface (amino acids 163–191) and the other in the C-terminus (amino acids 371–380, Fig. 1a, c). A similar analysis of rat TRESK also identified a shorter putative membrane-binding site in the large cytoplasmic loop, which aligned with that of the human channel (amino acids 198–207, Fig. 1b, c).

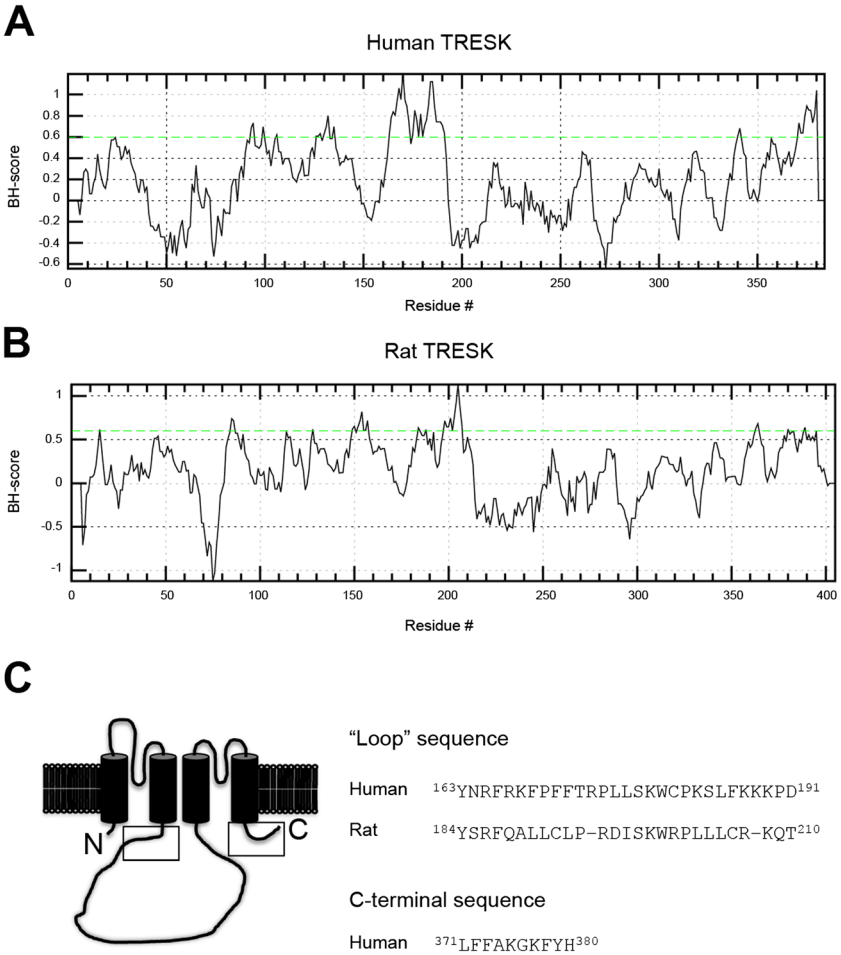

Fig. 1 In silico search for putative phospholipid binding sites in human and rat TRESK ($K_{2P}18.1$). The primary sequences of human (GenBank accession number NP_862823.1) and rat (GenBank accession number AAS68516.1) TRESK were analyzed using the BH search program. The threshold BH value for residues forming part of a potential membrane binding site was 0.6, and the search was performed with a window size of 10 to obtain scores for N- and C-terminal residues (Brzeska et al. 2010) [40]. **a** Results of the BH search analysis of human TRESK revealed two potential membrane binding sites between amino acids 163–191 and 371–380. **b** Results of the BH search analysis of rat TRESK, revealing one potential binding site between amino acids 198–207. **c** Schematic representation of TRESK with boxes indicating the positions of the identified lipid-binding sites. The amino acid sequences of the putative binding sites are shown alongside. In the case of the "loop" sequence, the human and rat sequences are aligned

The Intracellular Loop of Human TRESK Contains a Site for Binding to Anionic Phospholipids

To analyze whether the anionic phospholipid binding sites identified in our in silico analysis could mediate TRESK interaction with membrane lipids, we examined whether regions of human and rat TRESK containing these putative sites could bind to multilamellar vesicles (MLVs) composed of Folch fraction I lipids, an organic extract of bovine brain enriched in phosphoinositides and phosphatidylserine [49]. Stretches of the large intracellular loops of human (amino acids 163–244) and rat (amino acids 185–267) TRESK, as well as the short C-terminus of human TRESK (amino acids 356–384), were expressed in *E. coli* as fusions to glutathione-S-transferase (GST) (GST-hTRESK$_{(163–244)}$, GST-rTRESK$_{(185–267)}$, and GST-hTRESK$_{(356–384)}$, Fig. 2a). The purified GST fusion proteins were used in a liposome-binding assay based on pelleting of liposome-associated proteins, as shown in Fig. 2b. Under the conditions of our assay, appreciable pelleting of GST alone was not observed in the presence or absence of Folch Fraction multilamellar vesicles (Folch MLVs; Fig. 2c–e, lanes 1–4). The GST fusion proteins of the human and rat loops also did not show significant pelleting in the absence of Folch MLVs (Fig. 2c, d, lanes 5–6). Strikingly, in the presence of Folch MLVs, strong pelleting of GST-hTRESK$_{(163–244)}$ was observed (Fig. 2c, lanes 7–8) but not GST-rTRESK$_{(185–267)}$ (Fig. 2d, lanes 7–8). The GST fusion protein of the C-terminal portion of human TRESK, GST-hTRESK$_{(356–384)}$, showed significant pelleting in the absence and presence of Folch MLVs and was therefore not analyzed further (Fig. 2e, lanes 5–8). As shown in Fig. 2f, quantitative analysis of several experiments confirmed significantly

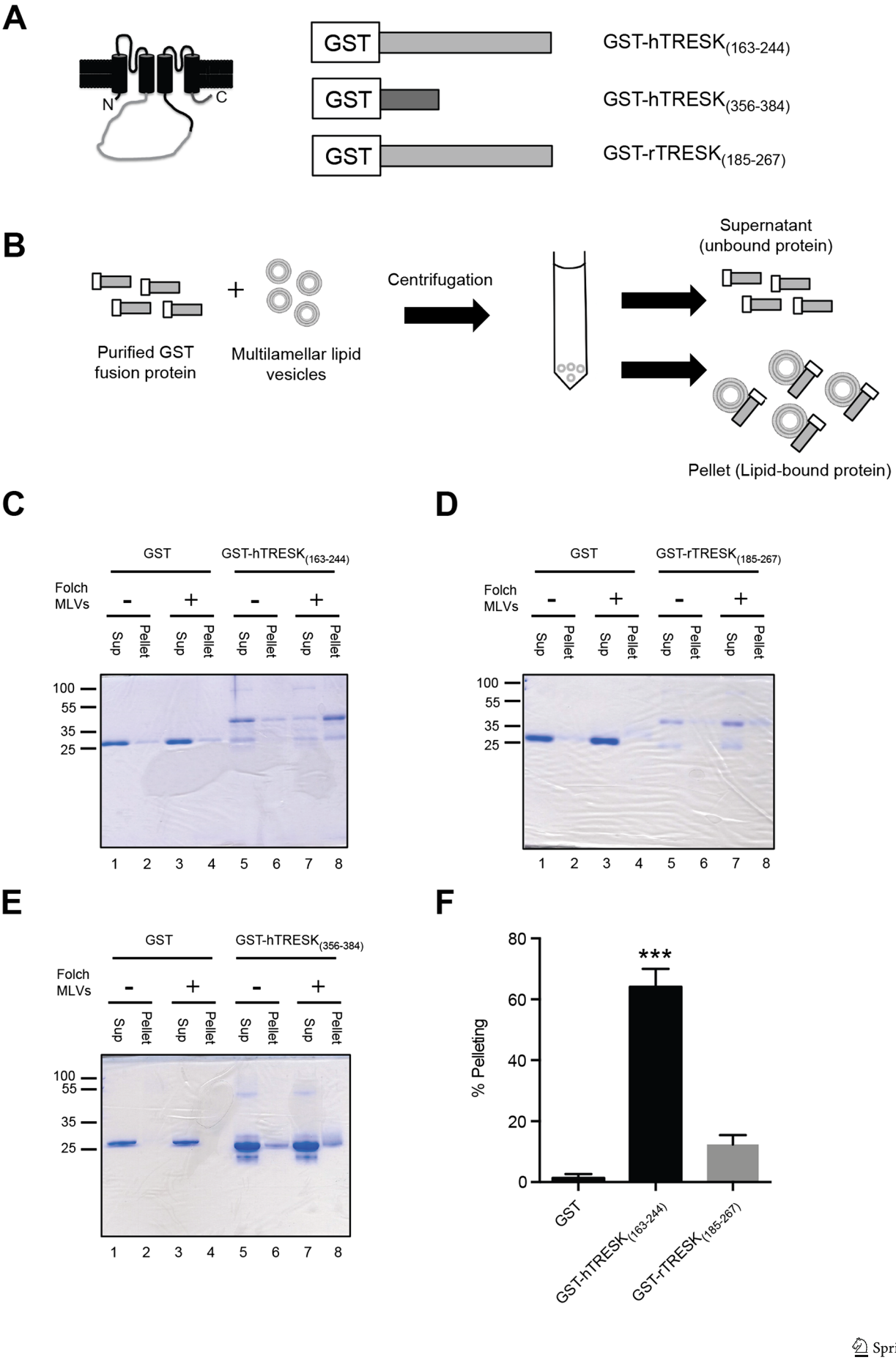
A
N
C
GST
GST-hTRESK(163-244)
GST
GST-hTRESK(356-384)
GST
GST-rTRESK(185-267)
B
Purified GST fusion protein
Multilamellar lipid vesicles
Centrifugation
Supernatant (unbound protein)
Pellet (Lipid-bound protein)
C
GST
GST-hTRESK(163-244)
Folch MLVs
Sup
Pellet
100
55
35
25
1 2 3 4 5 6 7 8
D
GST
GST-rTRESK(185-267)
E
GST
GST-hTRESK(356-384)
F
% Pelleting
***
GST
GST-hTRESK(163-244)
GST-rTRESK(185-267)

◀ **Fig. 2** Intracellular loop of human TRESK strongly binds to Folch Fraction Multilamellar Vesicles. **a** Schematic of the GST fusion proteins corresponding to the indicated regions of human and rat TRESK ($K_{2P}18.1$). The large intracellular loop and the C-terminus are shown in light and dark gray, respectively. **b** Summary of liposome binding assay methodology. Representative Coomassie-stained gels of liposome binding assays using purified GST-hTRESK$_{(163–244)}$ (**c**), GST-rTRESK$_{(185–267)}$ (**d**), and GST-hTRESK$_{(356–384)}$ (**e**). The positions of molecular weight standards (in kilodaltons) are indicated to the left of each gel. Lane numbers are indicated underneath the corresponding gels. **f** Quantification of the liposome binding assays showing the percentage of pelleting (mean ± SEM) after correction for the amount of pelleting in the absence of Folch MLVs. ***$p < 0.001$, Student's unpaired t test between GST-hTRESK$_{(163–244)}$ and GST-rTRESK$_{(185–267)}$

stronger pelleting of GST-hTRESK$_{(163–244)}$ (64.14 ± 5.84%, $n = 7$) compared to GST-rTRESK$_{(185–267)}$ (12.38 ± 3.06%, $n = 4$; $p < 0.001$, unpaired two-tailed t test). It should also be noted that both fusion proteins displayed significantly more pelleting than GST alone (GST pelleting = 1.4 ± 1.2%, $n = 9$; GST vs. GST-hTRESK $p < 0.0001$; GST vs. GST-rTRESK $p = 0.0017$, unpaired two tailed t tests). These in vitro observations demonstrate that the intracellular loop domain of human TRESK can interact with anionic phospholipids.

Folch Multilamellar Vesicles Activate Human TRESK Currents

After identification of the large intracellular loop of TRESK as a potential mediator of the interaction between the channel and anionic phospholipids, we went on to examine the functional consequences of disrupting electrostatic interactions between the channel and anionic phospholipids in the lipid bilayer. Cationic molecules, such as poly-lysine, interfere with electrostatic protein-lipid bilayer interactions by binding to and therefore "masking" negatively charged phospholipids [50]. Treatment with poly-cationic molecules produces inhibition of K^+ channels containing anionic phospholipid-binding domains [37, 51–53]. In HEK293 cells transfected with GFP-hTRESK and GFP-rTRESK, an initial application of poly-lysine (1 μg/ml) to the cytosolic side of inside-out patches produced significant current decreases of 35.8 ± 5.4% for hTRESK ($n = 7$; $p < 0.05$; Fig. 3d) and 36.9 ± 4.9% for rTRESK ($n = 4$; $p < 0.05$; Fig. 3d). The subsequent application of Folch Fraction Multilamellar Vesicles (MLVs) (10 μg/ml) to the cytosolic side of poly-lysine treated inside-out patches containing hTRESK produced a significant current activation of 125.5 ± 51.7% ($p < 0.001$; Fig. 3d). In contrast, almost no effect was found in rTRESK (12.1 ± 9.5%; $p = 0.101$; Fig. 3d). As a positive control, we assayed another K_{2P} channel previously shown to be modulated by anionic phospholipids, mouse TREK-1 ($K_{2P}2.1$) [37, 38]. mTREK-1 displayed similar behavior to hTRESK, displaying sensitivity to poly-lysine (% decrease 33.6 ± 4.8%; $n = 5$; $p < 0.01$; Fig. 3c, d) followed by subsequent activation by Folch Fraction MLVs (% increase 76.1 ± 22.3%; $p < 0.01$). As observed for hTRESK, a second application of poly-lysine produced a significant decrease in mTREK-1 current, reverting the previous lipid-mediated increase (Fig. 3b). It has been reported that membrane phospholipid binding of TREK-1 can modulate several properties of the channel, including voltage, stretch, and pH sensitivity [37]. We tested in inside-out patches whether hTRESK intracellular pH sensitivity was modified by the interaction between hTRESK and membrane phospholipids. As previously reported [8], acidic pH (from pH 7.2 to 5.5) decreased hTRESK current (45.1 ± 6.3%; $n = 5$; $p < 0.05$). Treatment with poly-lysine did not significantly modify the pH sensitivity of the channel (32.2 ± 10.4%; $n = 5$; $p = 0.335$). A similar result on pH sensitivity was obtained before and after treatment with Folch fraction (MLVs).

Our electrophysiological data demonstrated that the activity of TRESK is sensitive to poly-lysine treatment, suggesting that the disruption of electrostatic protein-bilayer interactions affects TRESK activity. However, when comparing the responses of rat and human TRESK to the application of Folch MLVs after poly-lysine treatment, important differences were observed. With rat TRESK, application of Folch MLVs restored poly-L-lysine inhibited currents to basal levels, presumably by sequestering the poly-L-lysine. However, with human TRESK, in addition to a sequestration effect, Folch MLVs potentiated channel activity above basal levels, which is likely to be due to an increase in the concentration of anionic phospholipids in the patch due to the incorporation of the Folch MLVs. The differential responses of human and rat TRESK to Folch MLVs are consistent with the presence of a stimulatory binding site for anionic phospholipids in human but not rat TRESK. The data from the liposome binding experiments shown in Fig. 2 suggest that this site may reside in the loop of human TRESK.

Mapping the Anionic Phospholipid Binding Site in the Cytoplasmic Loop of Human TRESK

The in silico analysis of human TRESK predicted that the site responsible for binding to anionic phospholipids resides between residues 163 and 191 (Fig. 1). Consistent with this, a GST-fusion protein containing this site showed significant interaction with Folch MLVs (Fig. 2c). On closer examination of the amino acid sequence of the putative anionic phospholipid-binding site, two separate clusters of positively charged amino acids could be distinguished. One of these clusters lies between amino acids 163 and 177 (^{163}YN**R**F**RK**FPFFT**R**PLL^{177}, denoted "Cluster 1" in Fig. 4a) and the other between amino acids 177 and 191 (^{177}LS**K**WCP**K**SLF**KKK**PD^{191}, denoted "Cluster 2" in Fig. 4a). We therefore designed GST fusion proteins to test whether one or both of these stretches were necessary for interaction with Folch MLVs. As previously shown (Fig. 2c), GST-hTRESK$_{(163–244)}$ pelleted strongly in the presence of Folch MLVs (Fig. 4b, left panel, lane 8 and Fig. 4c). Our analysis revealed that the fusion protein

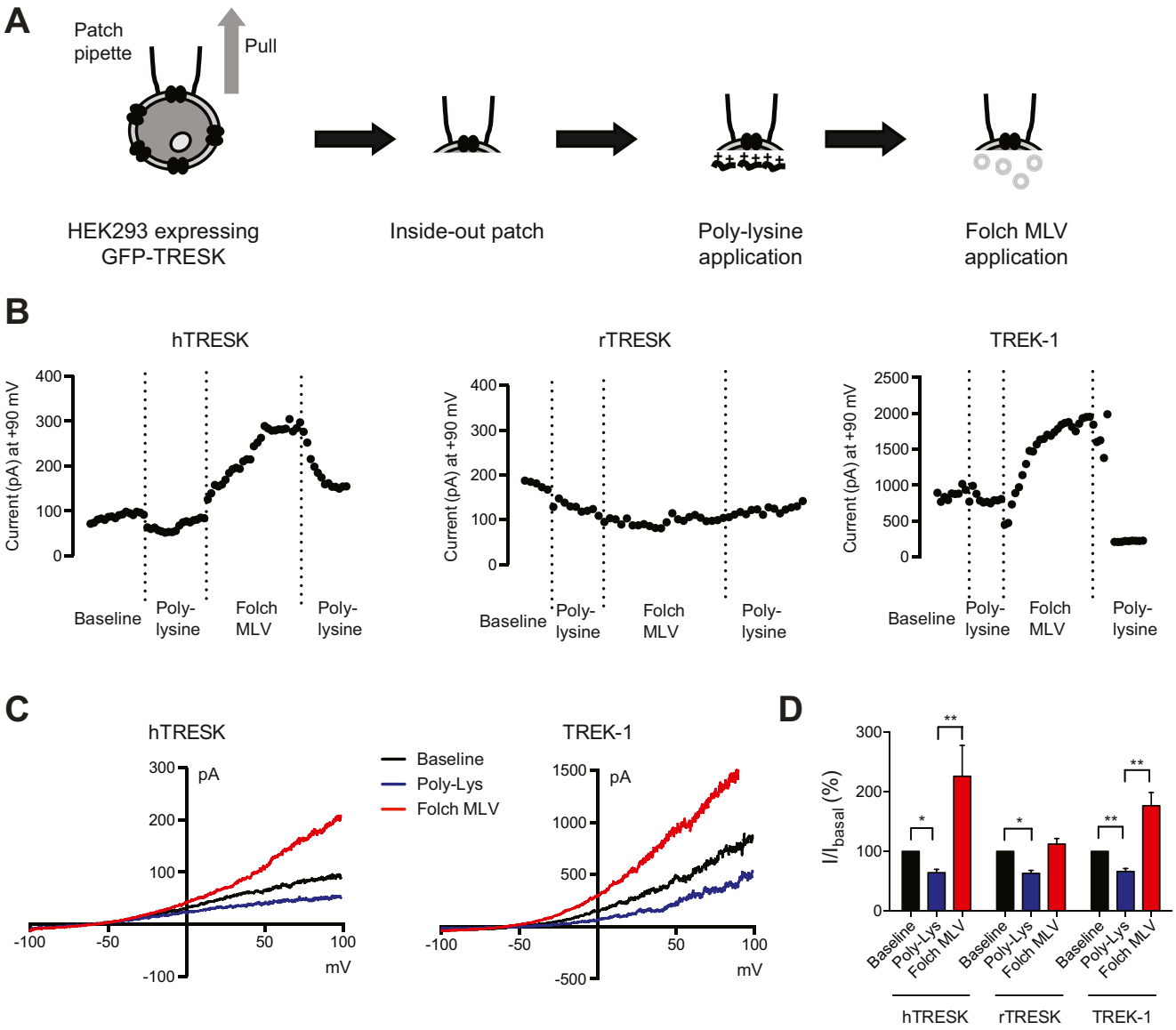

Fig. 3 Folch Fraction Multilamellar vesicles enhance human TRESK-mediated currents. **a** Schematic representation of the experimental protocol. **b** Representative time courses of human TRESK, rat TRESK, and mouse TREK-1 currents measured at + 90 mV from consecutive depolarizing ramps. From a holding voltage of − 80 mV, depolarizing ramps from − 100 to + 100 mV were recorded every 10 s on excised membrane patches in the inside-out configuration of the patch clamp technique. A physiological K^+ gradient was used (bath solution 140 mM K^+; pipette 5 mM K^+). Transfected HEK293 cells expressing GFP-hTRESK, GFP-rTRESK, and mTREK-1 were used. Poly-lysine and Folch MLVs were prepared in bath solution and applied at final concentrations of 1 and 10 μg/ml, respectively. **c** Representative currents elicited by depolarizing voltage ramps from − 100 to + 100 mV prior to (baseline) and during poly-lysine and Folch MLV application are shown. **d** Quantification of the experiments shown in panels **b** and **c**. GFP-hTRESK ($n = 6$), GFP-rTRESK ($n = 4$), and mTREK-1 ($n = 5$). *$p < 0.05$; **$p < 0.01$, Student's paired t test

containing "Cluster 1," GST-hTRESK$_{(163–207)}$, pelleted significantly with Folch MLVs (Fig. 4b, right panel, lane 4 and Fig. 4c; % pelleting = 64.6 ± 5.5%, $n = 3$). In contrast, the fusion proteins containing either only "Cluster 2" (GST-hTRESK$_{(177–244)}$) or neither cluster (GST-hTRESK$_{(187–244)}$) showed little or no pelleting with Folch MLVs (Fig. 4b, center panel and Fig. 4c; % pelleting = 9.2 ± 5.2%, $n = 4$ for GST-hTRESK$_{(187–244)}$ and 2.2 ± 2.2%, $n = 4$ for GST-hTRESK$_{(177–244)}$). These observations indicated that a stretch of 14 amino acids between residues 163 and 177 in human TRESK is necessary for interaction with Folch MLVs.

Testing the Role of the Phospholipid-Binding Cluster in the Cytoplasmic Loop of Human TRESK Using Human-Rat TRESK Chimeric Constructs

The liposome binding data shown in Fig. 4 strongly suggested that the stretch of amino acids between residues 163 and 177

of human TRESK is essential to mediate a physical interaction with anionic phospholipids. We then attempted to investigate the role of this stretch of amino acids in the modulation of TRESK activity by designing a series of chimeras between human and rat TRESK. It is interesting to note that alignment of the anionic phospholipid binding stretch we have identified in human TRESK with the corresponding sequence in rat TRESK revealed significant differences (Fig. 5a). These differences may explain why the loop of human TRESK displays a much stronger binding to Folch MLVs compared to the rat loop (see Fig. 2). Of the four positively charged residues in the human stretch, only two are conserved in the rat sequence (R186 and R195). Furthermore, there is an aspartate residue in the rat sequence (D196), which at physiological intracellular pH would be negatively charged and therefore likely to interfere with anionic phospholipid-based interactions. As shown in Fig. 5b, two chimeras between human and rat TRESK were initially constructed. In the first chimera, the large intracellular loop, the third and fourth transmembrane domains of hTRESK were replaced with the corresponding sequence from rTRESK (hTRESK-rat-loop-rTRESK). A complementary second chimera was constructed in the same way (rTRESK-human-loop-hTRESK). The effects of poly-L-lysine followed by Folch MLV application to inside-out patches of HEK293 cells expressing each chimera were tested. In both cases, no significant effects of either poly-L-lysine or Folch MLVs on channel currents were observed (Fig. 5c).

A second set of chimeras was also tested where only the anionic phospholipid binding site (apbs) from human TRESK replaced the equivalent sequence in rat TRESK (rTRESK-h-apbs) or vice versa (hTRESK-r-apbs). The effects of poly-L-lysine followed by Folch MLV application to inside-out patches of HEK293 cells expressing each chimera were tested. As expected from liposome binding data in Fig. 2, replacement of the apbs in hTRESK by the rat sequence produced a chimeric channel unresponsive to poly-lysine ($-6.0 \pm 7.2\%$, $n = 7$) or Folch MLV application ($5.7 \pm 5.2\%$, $n = 7$; Fig. 5d, e). In agreement, a GST-r-apbs-hloop construct showed significantly less binding to Folch MLVs (21% pelleting; data not shown) compared to the normal human loop sequence (Fig. 2), providing further evidence for the importance of the human apbs in mediating interaction with anionic phospholipids. In contrast, when the apbs in rTRESK was replaced by the human one, the channel acquired responsiveness to poly-lysine ($-10.0 \pm 8.9\%$, $n = 11$; $p < 0.05$) and was potentiated by Folch MLV application ($128.7 \pm 45.2\%$, $n = 11$; $p < 0.05$; Fig. 5d, e), similarly to what was observed in the wild-type human channel.

The results of this analysis suggest that the apbs of hTRESK is sufficient to confer modulation by anionic phospholipids on rTRESK. However, in those chimeras where larger portions of each ortholog were switched (the rTRESK-human-loop-hTRESK and hTRESK-rat-loop-rTRESK chimeras), modulation by poly-lysine and Folch MLVs was lost. This suggests that these chimeras had an altered channel tertiary structure resulting in disrupted channel gating and/or there are other elements in the human TRESK structure that can interfere with the stimulatory function of the apbs.

The Intracellular Loop of Human TRESK Binds to Liposomes Enriched with Phosphatidylserine and Phosphatidylinositol-4,5-Bisphosphate (PIP_2)

To determine whether the human TRESK intracellular loop displayed preferential binding for a particular type of anionic phospholipid and to further analyze potential differences between the lipid binding characteristics of the rat and human loops, we performed pelleting experiments using multilamellar liposomes of defined composition. GST-$hTRESK_{(163–244)}$ pelleted strongly in the presence of liposomes enriched with anionic phospholipids, either 50% phosphatidylcholine (PC)/50% phosphatidylserine (PS) (Fig. 6a, lane 6) or 70% phosphatidylcholine/25% phosphatidylserine/5% phosphatidylinositol-4,5-biphosphate (PIP_2; Fig. 6a, lane 8) but did not show significant pelleting with liposomes composed solely of the neutral lipid PC (Fig. 6a, lane 4). Quantification of pelleting from three independent experiments showed significant differences between PC-only liposomes and those enriched with anionic phospholipids (PS and PIP_2). However, no difference in pelleting was observed between the two types of liposomes enriched with anionic phospholipids (PS vs PIP_2) (Fig. 6c). In contrast, GST-$rTRESK_{(185–267)}$ did not show specific pelleting with any of the liposomes tested (Fig. 6b, lanes 4, 6, and 8). We attempted to further characterize the lipid specificity of the human TRESK loop using commercially available strips spotted with various types of lipid (PIP strips from Thermo Fisher Scientific). However, no firm conclusions could be drawn due to a high level of GST binding to lipid spots (data not shown). The results of these liposome-pelleting experiments indicate that the intracellular loop of human TRESK contains a binding site for anionic phospholipids that does not display a preference for a specific lipid type.

PIP_2 Enhances Human TRESK Currents

It is likely that the anionic phospholipid-binding site in the large cytoplasmic loop of human TRESK will bind preferentially to the phosphoinositide $PI(4,5)P_2$ under physiological conditions in native plasma membranes, on the basis of its trivalency at pH 7 and its concentration in the plasma membrane (approximately 1% of total lipid). In addition, physiologically relevant changes in plasma membrane $PI(4,5)P_2$ concentration can occur during $G_{q/11}$-coupled receptor stimulation by agonists such as hormones and neurotransmitters [54]. Therefore, we tested the effect of adding a water-soluble form of $PI(4,5)P_2$ (diC8:0 $PI(4,5)P_2$) to inside-out patches taken from HEK293 cells

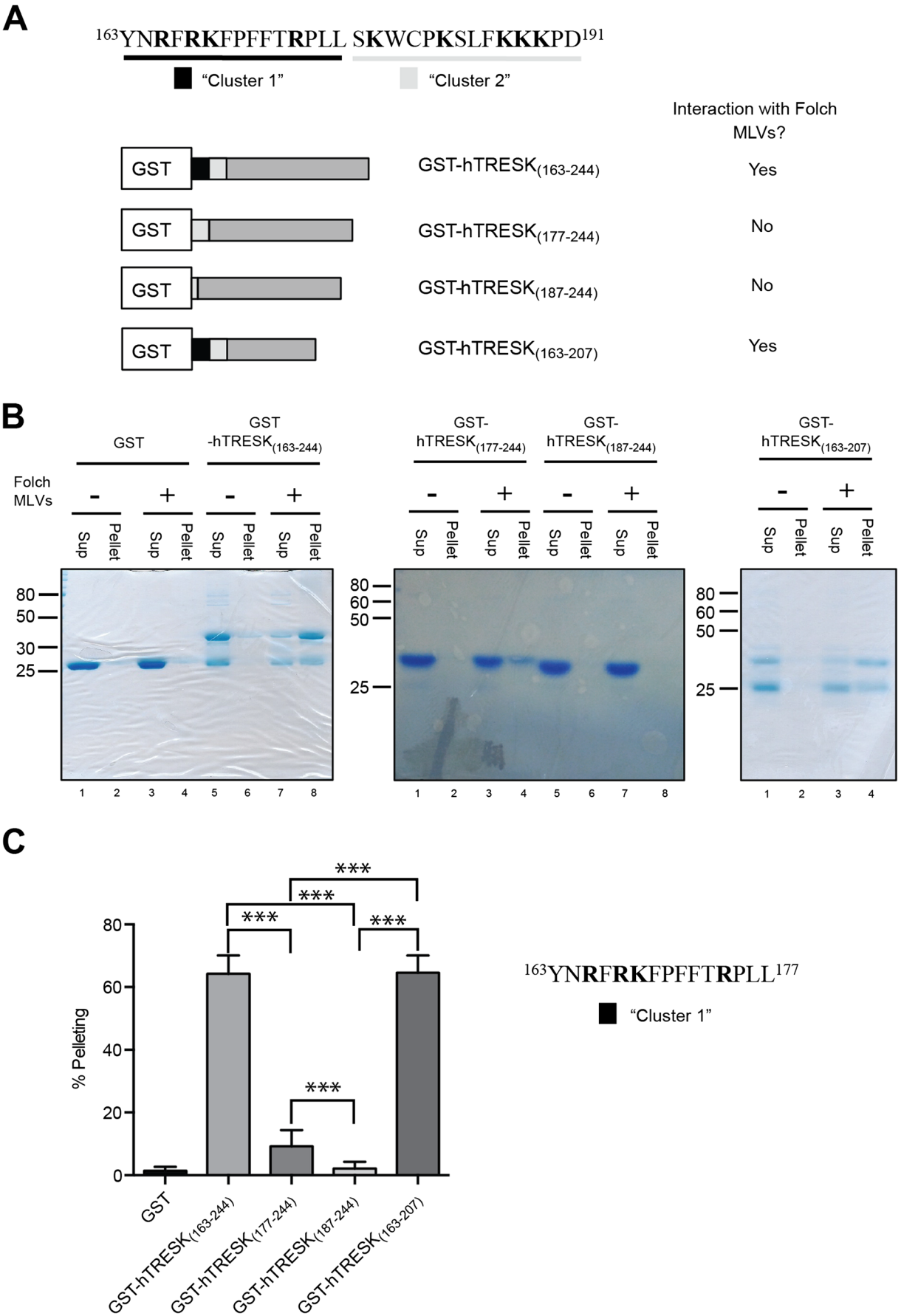
A
163YNRFRKFPFFTRPLL SKWCPKSLFKKKPD191
"Cluster 1"
"Cluster 2"
Interaction with Folch MLVs?
GST
GST-hTRESK(163-244)
Yes
GST
GST-hTRESK(177-244)
No
GST
GST-hTRESK(187-244)
No
GST
GST-hTRESK(163-207)
Yes
B
GST
GST -hTRESK(163-244)
GST-hTRESK(177-244)
GST-hTRESK(187-244)
GST-hTRESK(163-207)
Folch MLVs
Sup
Pellet
80
60
50
30
25
1 2 3 4 5 6 7 8
C
% Pelleting
***
GST
GST-hTRESK(163-244)
GST-hTRESK(177-244)
GST-hTRESK(187-244)
GST-hTRESK(163-207)
163YNRFRKFPFFTRPLL177
"Cluster 1"

◀ **Fig. 4** A short stretch of amino acids in the cytoplasmic loop of human TRESK determines the anionic phospholipid binding. **a** Schematic representation of the GST fusion proteins corresponding to different portions of the large cytoplasmic loop of human TRESK. The amino acid sequences of the two "clusters" containing groups of positively charged amino acids are also indicated, with the numbers denoting the position in the primary sequence of human TRESK. "Cluster 1" (amino acids 163 and 177) and "Cluster 2" (amino acids 178–191) are indicated by the black and gray squares, respectively, on the fusion protein schematics. **b** Representative Coomassie-stained polyacrylamide gels of liposome binding assays. Left panel, results of a control experiment (shown for comparison) performed with GST and GST-hTRESK$_{(163–244)}$ similar to the one shown in Fig. 2c. Centre panel, results of experiments with the fusion proteins GST-hTRESK$_{(177–244)}$ and GST-hTRESK$_{(187–244)}$. Right panel, results of a representative experiment performed with the GST-hTRESK$_{(163–207)}$ fusion protein. **c** Quantitative summary (% pelleting; mean ± SEM; $n = 3–4$ independent experiments per group) of the liposome binding assays showing percentage of pelleting after correction for the amount of pelleting in the absence of Folch MLVs. ***$p < 0.001$, Student's unpaired t test

transiently expressing hTRESK. As displayed in Fig. 7a, b, in a similar fashion to Folch MLVs, diC8:0 PI(4,5)P_2 (5 μM) produced a significant activation of hTRESK previously inhibited by 1 μg/ml poly-L-lysine in seven out of nine patches tested (% increase 99.9 ± 39.8%, $n = 7$; $p < 0.05$; Fig. 7c), while no effect was found in two additional patches. To assess if the membrane lipid binding is specific for PI(4,5)P_2 or just for anionic lipids, we tested the effect of PI(4,5)P_2 hydrolysis by the *Ciona intestinalis* voltage sensing phosphatase (CiVSP) as previously assayed for TREK-1 [55, 56]. Whole cell recordings in HEK293 cells expressing hTRESK with or without CiVSP did not show significant differences in the current activated by voltage ramps (− 100 to + 50 mV) before and after a prepulse (+ 150 mV, 200 ms) to activate the phosphatase (% inhibition: hTRESK 0.77 ± 5.0%, $n = 4$; hTRESK+CiVSP 12.6 ± 12.8%, $n = 5$; $p = 0.326$).

As previously described, changes in membrane PI(4,5)P_2 concentration after activation of GPCRs modulate the activity of several ion channels and membrane proteins [31, 32, 57–59]. It is well-known that TRESK is modulated by changes in intracellular Ca^{2+} through dephosphorylation by calcineurin [27]. In view of our results, we explored the possibility that a dual regulation of hTRESK by PIP_2 and Ca^{2+}/calcineurin might exist. To address this, we cotransfected hTRESK and mGluR5 (a metabotropic glutamate receptor that can activate phospholipase C) in HEK293 cells and recorded hTRESK current in whole-cell experiments. To dissociate the possible effect of PI(4,5)P_2 concentration changes from the Ca^{2+}-mediated modulation of hTRESK current, we included EGTA to chelate any free Ca^{2+} and FK-506 to block calcineurin activity. Under these conditions, stimulation of mGluR5 with 50 μM glutamate produced a significant decrease in hTRESK current (− 38.2 ± 7.9%, $n = 8$; $p < 0.001$; Fig. 7d, f) likely due to PIP_2 hydrolysis. In contrast, HEK293 cells transfected only with hTRESK did not show significant changes in whole-cell current after stimulation with glutamate (control, Fig. 7f). Finally, to evaluate the relative contributions of the lipid- and Ca^{2+}-modulatory effects on hTRESK, we performed experiments in HEK293 cells co-expressing mGluR5 and hTRESK in the cell-attached configuration of the patch-clamp technique, thus preserving native cytoplasmatic conditions. Glutamate application produced an overall increase in hTRESK current (38.9 ± 12.2%, $n = 12$; $p < 0.05$; Fig. 7e, left and 7f), consistent with previous reports [29, 60]. This indicates that, at least after stimulation of mGluR5 receptors, the activating effect of Ca^{2+}/calcineurin is more important than the lipid-mediated inhibition. Interestingly, in 50% of the recordings (6 of 12), a biphasic effect was observed: an initial and transient increase in TRESK current followed by a sustained decrease (− 27.5 ± 6.6%, $n = 6$), which could reflect an initial stimulatory effect of Ca^{2+}/calcineurin on hTRESK followed by hydrolysis of PIP_2 at the plasma membrane (Fig. 7e, right). Nevertheless, some variability existed on the current increase/decrease observed that would reflect a competition between opposing modulatory mechanisms. An additional experiment in the same configuration (cell-attached) was performed in HEK293 cells co-transfected with hTRESK and hTRPA1 in order to determine the effect on hTRESK resulting from activation of a receptor/channel not linked to G-protein-mediated phospholipase C activation and membrane lipid hydrolysis but that its activation increases intracellular Ca^{2+}. In these conditions, allyl isothiocyanate (AITC; 100 μM), a well-known activator of TRPA1, produced a significant increase in hTRESK current (170.6 ± 29.3%, $n = 6$; $p < 0.01$; Fig. 7f, right), but no decrease in the current was observed. As a control, in HEK293 cells transfected only with hTRESK, AITC did not produce any significant change on the recorded current (− 13.1 ± 6.4%, $n = 4$).

Discussion

In this study, we present evidence that argues for a species-specific modulation of TRESK by anionic phospholipids, requiring a juxtamembrane region in the large intracellular loop of the channel. It is well established that other members of the K_{2P} family (TREK-1, -2, TASK-1, -3) are activated by anionic phospholipids, with changes in local PIP_2 concentration appearing to be particularly important modulating factor [37–39, 61, 62]. In the case of TREK-1 (K_{2P}2.1), a short sequence of amino acids acts as a type of "phospholipid sensor" that links channel activity to PIP_2 concentration changes [37]. We used an in silico approach to identify regions in TRESK that could fulfill a similar role (Fig. 1). After identifying potential interacting regions, we used a liposome-binding assay to test their ability to bind to multilamellar vesicles enriched with anionic phospholipids (Folch fraction liposomes). These experiments revealed that, somewhat surprisingly, there appeared to be a difference in the ability of equivalent portions of the large cytoplasmic loop domain from

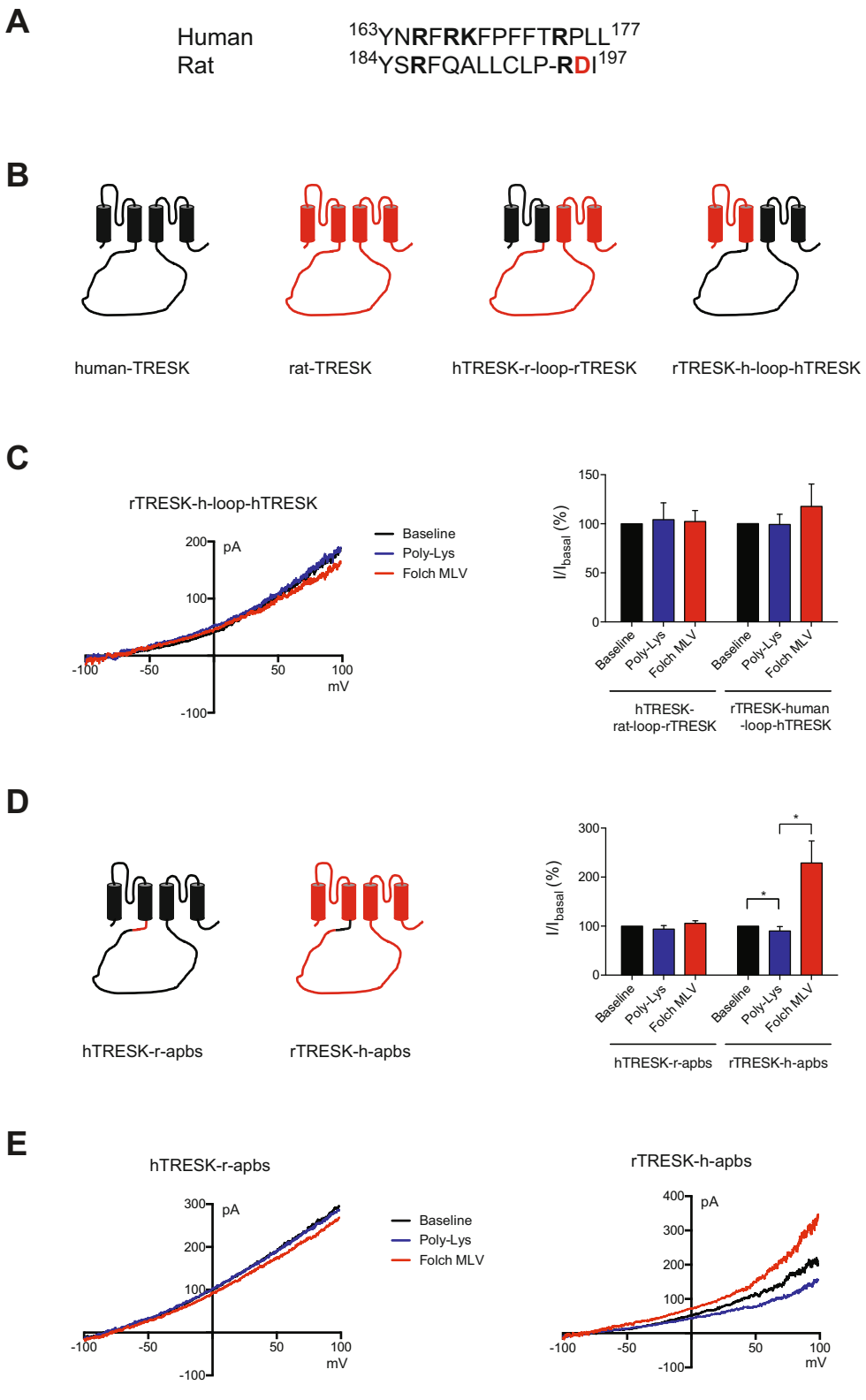

different TRESK orthologues to bind to anionic phospholipids. The region identified in the loop domain of hTRESK exhibits a much stronger binding to anionic phospholipids compared to the equivalent region in rat TRESK, probably due to the presence of a cluster of four positively charged residues in the human stretch, while only two are conserved in the rat sequence (R186 and R195, see Fig. 5a). Additionally, the identified region in the rat contains a

◀**Fig. 5** The anionic phospholipid binding site of human TRESK can confer stimulation by Folch MLVs on rat TRESK. **a** Comparison of the anionic phospholipid binding site (apbs) identified in human TRESK and the equivalent sequence in rat TRESK. **b** Representation of the human, rat, and human/rat chimeric TRESK channels tested. **c** Left: representative currents elicited by depolarizing voltage ramps from − 100 to + 100 mV prior to (baseline) and during poly-lysine (1 μg/ml) and Folch MLV (10 μg/ml) application are shown in the rTRESK-h-loop-hTRESK chimeric channel. Recordings were performed in inside-out membrane patches in a physiological K^+ gradient (bath solution 140 mM K^+; pipette 5 mM K^+). Right: quantification of the experiments in hTRESK-rat-loop-rTRESK ($n = 5$) and rTRESK-human-loop-hTRESK ($n = 6$) chimeric channels. Currents were measured at + 90 mV from depolarizing ramps such as the example shown on the left. **d** Left: chimeric channels where the anionic phospholipid binding site (apbs) in human TRESK was replaced by the equivalent sequence from rat (hTRESK-r-apbs) or vice-versa (rTRESK-h-apbs). Right: quantification of the experiments in hTRESK-r-apbs ($n = 7$) and rTRESK-h-apbs ($n = 11$) chimeric channels. Currents were measured at + 90 mV from depolarizing ramps, examples of which are shown in panel **e**. **e** Representative currents elicited by depolarizing voltage ramps from − 100 to + 100 mV prior to (baseline) and during poly-lysine and Folch MLV application are shown for the hTRESK-r-apbs and rTRESK-h-apbs chimeric channels. Recordings were performed in inside-out membrane patches in a physiological K^+ gradient. *$p < 0.05$; Student's paired t test

negatively charged aspartate residue (D196), which would be likely to interfere with any interaction with anionic phospholipids. We did not test the mouse TRESK orthologue, but analysis of its sequence shows that only one positive residue is present in the equivalent domain and it also contains the same negative residue present in rat, which probably makes unlikely an interaction with membrane lipids. In contrast to TREK-1 where the lipid-binding protein sequence resides in the C-terminal domain of the channel, evaluation of another possible lipid-binding sequence in the C-terminal domain of human TRESK did not show significant specific binding to Folch fraction liposomes. This further underlies the important regulatory role of the large intracellular loop of TRESK between transmembrane domains 2 and 3. For instance, several protein-protein interaction sites and phosphorylation motifs are present in this domain [27, 28, 60, 63–65], which exerts a similar role to the C-terminal domain in TREK-1. Changes in this lipid-binding domain such as the reduction in the number of positively charged amino acid residues and the presence of negatively charged residues (as occurs in the rat channel) appear to be critical for membrane lipid binding. This physical interaction does not appear to be important for the control of channel gating since human and rodent channels show similar activation profiles. However, it does seem to be important for "fine-tuning" of channel regulation.

Binding assays using liposomes with defined lipid compositions revealed that the loop domain of hTRESK bound to liposomes enriched with anionic phospholipids such as phosphatidylserine and PIP_2 but not to liposomes composed solely of the neutral phospholipid, phosphatidylcholine. Several ion channels and, in particular, potassium channels

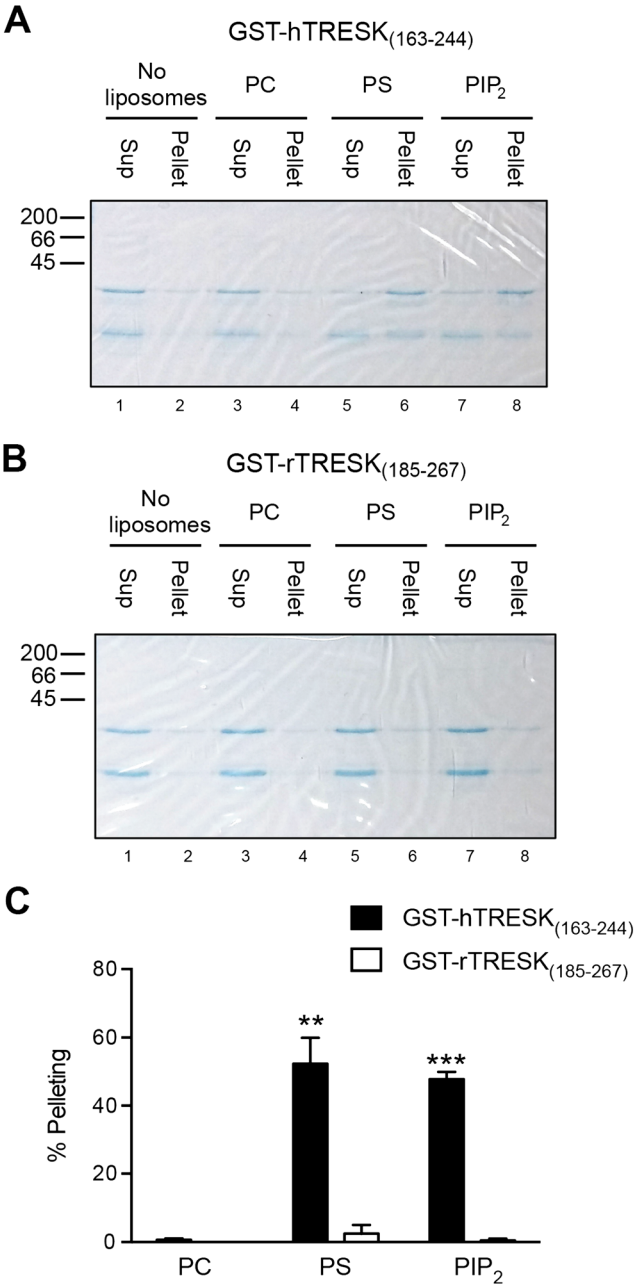

Fig. 6 Differential binding of the intracellular loops of human and rat TRESK to liposomes enriched with phosphatidylserine and phosphatidylinositol-4,5-bisphosphate (PIP_2). Coomassie-stained gels of representative liposome-binding assays with purified GST fusion proteins corresponding to equivalent portions of the large intracellular loop of human TRESK (amino acids 163–244) (**a**) and rat TRESK (amino acids 185–267) (**b**). The liposome compositions were (mole % in brackets) as follows: PC = phosphatidylcholine (100%); PS = phosphatidylcholine (50%)/phosphatidylserine (50%); PIP_2 = phosphatidylcholine (70%)/phosphatidylserine (25%)/phosphatidylinositol-4,5-bisphosphate (5%). **c** Quantitative summary (% pelleting; mean ± SEM) of three independent experiments for GST-$hTRESK_{(163–244)}$ and GST-$rTRESK_{(185–267)}$ showing the percentage of pelleting after correction for the amount of pelleting in the absence of liposomes. **$p < 0.01$; ***$p < 0.001$, Student's unpaired t test vs. pelleting in the presence of PC-only containing liposomes

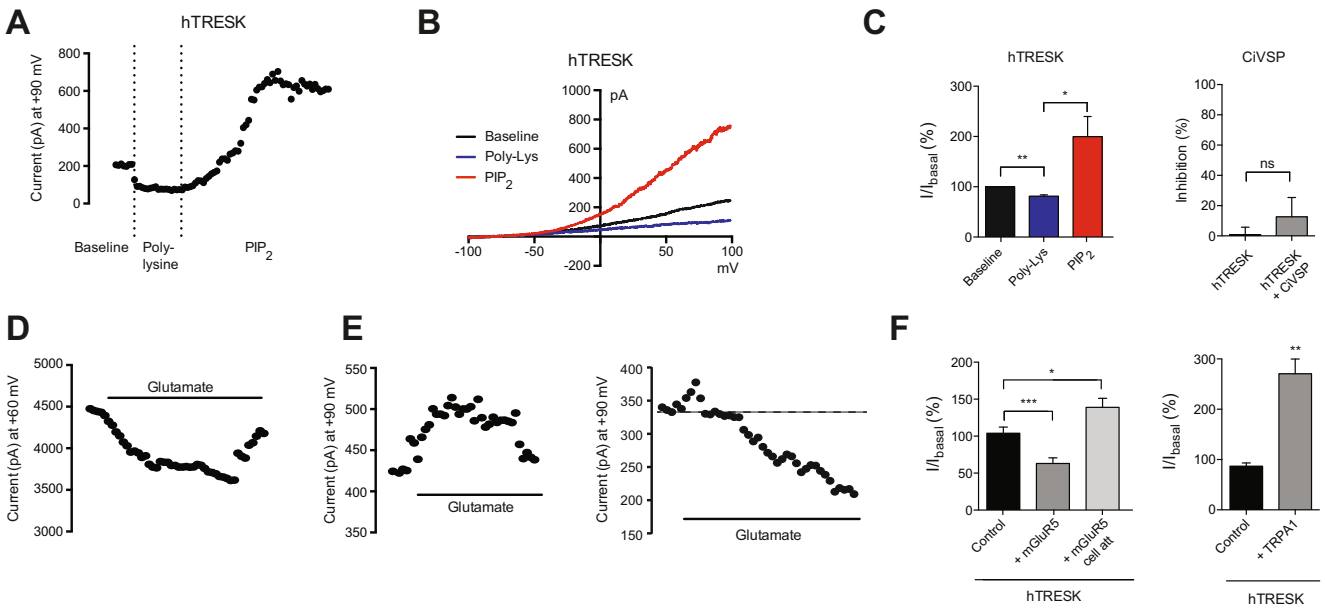

Fig. 7 PIP_2 enhances human TRESK-mediated currents. **a** Representative time course of human TRESK currents measured at + 90 mV from consecutive depolarizing ramps. In transfected HEK293 cells expressing GFP-hTRESK, depolarizing ramps from − 100 to + 100 mV were recorded every 10 s (holding voltage − 80 mV) on excised membrane patches in the inside-out configuration of the patch clamp technique. A physiological K^+ gradient was used (bath solution 140 mM K^+; pipette 5 mM K^+). The effects of adding poly-lysine (1 μg/ml) and a water-soluble form of $PI(4,5)P_2$ (diC8:0 $PI(4,5)P_2$) (5 μM) to the bath solution (cytosolic side of the patch) on TRESK currents were measured. **b** Representative currents elicited by depolarizing voltage ramps from − 100 to + 100 mV prior to (baseline), during poly-lysine and PIP_2 application are shown. **c** Left: quantification of the experiments shown in panels **a** and **b** GFP-hTRESK ($n = 7$). Right: quantification of the effect on hTRESK current of PIP_2 hydrolysis by activation of CiVSP phosphatase. hTRESK ($n = 4$); hTRESK+CiVSP ($n = 5$). $^*p < 0.05$; $^{**}p < 0.01$, Student's paired t test. **d** Representative time course of human TRESK currents in transfected HEK293 cells expressing GFP-hTRESK and mGluR5. Current was measured at + 60 mV from consecutive depolarizing ramps from − 100 to + 60 mV recorded every 10 s (holding voltage − 60 mV) in the whole-cell configuration of the patch clamp technique. A physiological K^+ gradient was used. The pipette solution contained EGTA and the calcineurin blocker FK-506. Glutamate (50 μM) was added to the bath as indicated. **e** Left: representative time course human TRESK currents in transfected HEK293 cells expressing GFP-hTRESK and mGluR5. Current was measured at + 90 mV from consecutive depolarizing ramps from − 100 to + 100 mV recorded every 10 s (holding voltage 0 mV) in the cell-attached configuration of the patch clamp technique. Both the bath and the pipette contained a physiological solution. Glutamate (50 μM) was added in the bath as indicated. Right: example of a recording showing increasing and decreasing effects on hTRESK current. **f** Left: quantification of the experiments shown in panels **d** and **e**. Cells transfected only with GFP-hTRESK (control; $n = 7$); whole-cell recordings in GFP-hTRESK+ mGluR5 cells ($n = 8$); cell-attached recordings in GFP-hTRESK+ mGluR5 cells ($n = 12$). Right: quantification of the effect of TRPA1 activation (AITC 100 μM) on hTRESK current in HEK293 cells transfected only with hTRESK ($n = 4$) or with hTRESK+hTRPA1 ($n = 6$). $^*p < 0.05$; $^{**}p < 0.01$; $^{***}p < 0.001$, Student's paired t test

including K_{ir}, K_v, KCNQ, and K_{Ca} are regulated by phosphoinositides, including PIP_2 (for review see [66]). In fact, other channels of the K_{2P} family are regulated by different phospholipids as well as by PIP_2 [37–39, 67–69]. Here, we found that exogenous PIP_2 increased hTRESK activity in isolated inside-out patches. A closer inspection of the putative anionic phospholipid-binding region in hTRESK revealed the presence of two "clusters" of positively charged amino acids, which may be responsible for mediating binding to anionic phospholipids. We tested the role of these clusters in phospholipid binding using the liposome binding assay and determined that only one of these clusters is necessary to mediate binding to anionic phospholipids (Fig. 4). However, there is a possible smaller contribution from cluster 2 as the GST-$hTRESK_{(177–244)}$ shows significant binding above GST and significantly more than the fusion protein lacking both clusters, GST-$hTRESK_{(187–244)}$. Rat TRESK seems to have cluster 2, which may explain the residual binding activity observed in the pelleting assay (Fig. 2f).

In our experiments, hTRESK is able to bind to PIP_2 to increase the channel current. In TREK-1, it has been described that when endogenous phospholipids are "quenched" by poly-cationic poly-lysine, mechano-sensitivity is significantly reduced [37]. Also, PIP_2 exerts a dual regulation of TREK-1 activation by intracellular pH (pHi) or mechanical stimuli. In the presence of PIP_2, mechanosensitivity or activation by pHi is reduced, but in the presence of poly-lysine, the effects are reverted and PIP_2 can promote activation of the channel [37–39]. TRESK is not directly activated but modulated by membrane stretch or by changing membrane curvature [21], in contrast to TREK-1 or -2 that can be directly activated by mechanical stimuli. It remains to be explored if stretch modulation of hTRESK current is enhanced or diminished by the binding to membrane phospholipids. Another possibility is

that changes in the intracellular pH (pHi) might produce protonation of some residues to modify the interaction with membrane lipids. In TREK-1 channels at acidic pHi, exogenous phospholipids transform the mechano-gated channel into a K^+-selective leak conductance [37]. Also, blocking the interaction between the C-terminal domain and membrane lipids by addition of poly-lysine abolishes activation by acidic pHi [37, 38]. In hTRESK, acidic pHi produces the opposite effect and decreases the current, while alkalinization increases it [8]. We tested whether hTRESK intracellular pH sensitivity was modified by the interaction with membrane lipids, but no significant differences were found, indicating that at least intracellular pH sensitivity is not dependent on this interaction, in contrast to what occurs for TREK-1. Whether other biophysical properties of the channel are affected by the binding to membrane lipids remains to be studied.

Other K_{2P} channels are modulated by hormones and neurotransmitters through activation of different GPCRs linked to G_s-cAMP-PKA phosphorylation, G_q-PLC-DAG-PKC phosphorylation, or PIP_2 membrane depletion (for review see [3]). Interestingly, TRESK is the only member of the family regulated by Ca^{2+}/calcineurin dephosphorylation, which increases the channel current [27]. Therefore, by increasing the cytosolic Ca^{2+} through membrane ion channels or after stimulation of $G_{q/11}$-coupled receptors and Ca^{2+} release from internal stores results in TRESK activation [27, 29, 30]. However, the net stimulation is likely to be the sum of two consequences of receptor activation: a Ca^{2+}-dependent activation of TRESK by calcineurin and an inhibition due to PIP_2 hydrolysis in the vicinity of the channel. Here, we show that activation of a membrane GPCR linked to $G_{q/11}$ activation and Ca^{2+} release (mGluR5) produces a significant decrease in channel current that is likely due to PIP_2 hydrolysis when the Ca^{2+}-mediated effects are blocked (calcium-chelating buffer+inhibitor of calcineurin). In contrast, when both modulatory mechanisms can be activated, the overall effect in the majority of the cells is an increase of hTRESK current, indicating that the Ca^{2+}/calcineurin effect predominates, although in some cells, a biphasic effect is observed. In this sense, stimulation of TRPA1, a receptor/channel that produces an intracellular Ca^{2+} increase but is not linked to G-protein activation and phospholipid hydrolysis, produced a bigger effect on hTRESK since it is only activating one of the modulatory mechanisms.

During inflammation or nerve injury, a mix of chemicals is released producing the sensitization of nociceptive sensory neurons and contributing to chronic pain [70]. These chemicals, in many cases, activate pronociceptive GPCRs [70, 71]. Because many pronociceptive receptors signal through PLC (and require PIP_2 for signaling), the modulation of hTRESK by membrane lipids might be relevant. Enhancing effects of Ca^{2+} on TRESK current have been described after stimulation with several neurotransmitters or inflammatory mediators such as bradykinin, 5-HT, glutamate, lysophosphatidic acid (LPA), histamine, or muscarinic agonists [29, 30, 60]. All these studies used rodent (mostly mouse) TRESK orthologs where the Ca^{2+}-calcineurin-mediated TRESK activation would be more prominent due to the lack of lipid binding and regulation. In contrast, in the human channel, a combination of both effects will be present. Depending on the receptor activated and the PIP_2 hydrolysis in restricted membrane microdomains, the excitatory or inhibitory effects on TRESK could prevail. In fact, several differences have been reported between the rat/mouse and human TRESK channels, including the sensitivity to anesthetics (higher enhancing efficacy to isoflurane and less blocking effect of lidocaine in hTRESK) [72], the docking of calcineurin to the channel, and their sensitivity to Ca^{2+} regulation [73] or the sensitivity to Zn^{2+} ions and pH [72, 74]. The fact that human and rodent coding sequences share only about 65% identity and 71% overall amino acid similarity is likely to be the reason for this different modulatory effect, including the lipid regulation described here. These species differences must be taken into consideration when extrapolating pharmacological results from rodent experimental models to human physiology or during drug development.

It has been proposed that in sensory neurons, TRESK counteracts membrane depolarization induced by external stimuli or diverse chemical substances in order to prevent excessive neuronal activation [3, 10, 11, 17, 30]. A recent report shows combined enhancement of TRESK and TRPV1 currents by LPA, an inflammatory mediator, with potentiation of hyperpolarizing TRESK currents counteracting to some extent the depolarizing effects derived from TRPV1 [30]. In fact, TRESK seems to be modulated by different stimuli, including Ca^{2+}, membrane curvature, or arachidonic acid [8, 21, 27]. As an example, during inflammation, both LPA, arachidonic acid, and hypertonic conditions can be present, the first one enhancing TRESK current while the latter two decrease TRESK current [21, 30]. It is worth considering that, at least for the human channel, while activation of GPCRs will produce a modulation of TRESK current through membrane lipids and by Ca^{2+}/calcineurin, activation of TRESK via Ca^{2+} influx through direct activation of membrane channels such as TRPV1 or TRPA1 will only produce a potentiation of the current, as shown in experiments where TRPA1 was activated. This would suggest that depending on the stimuli activating the sensory neuron, the role of TRESK counterbalancing the depolarizing effect of the stimulus might be different. Taken together, it appears that depending on the stimuli, TRESK can be modulated negatively or positively and the final amount of hyperpolarizing current counterbalancing depolarization might vary in different situations. Here, we show that membrane lipids also contribute to this regulation, at least in the human channel. In addition, regulation of TRESK expression is another factor to be added into the equation, since injury or inflammation produce a down-regulation of the channel

expression [10, 75]. Because TRESK represents a common regulation point by all these stimuli, it can be postulated as an interesting way to bypass the membrane receptor diversity and to target a point where different signaling pathways converge. In this way, analgesic drug development to enhance TRESK activity could be an interesting approach to treat pain.

In summary, here, we describe a novel regulation of human TRESK by anionic membrane lipids through interaction with a motif in the intracellular loop of the channel. This regulation is unique in the human channel and not present in rodent orthologs. This finding further expands the different properties of the human channel, which should be taken into account when extrapolating results from rodent models. Also, it opens the door to possible new drug developments that target this channel for the treatment of pain.

Authors' Contributions Authors JPG, AC, and AA carried out cellular cultures, plasmid generation, and transfection. JPG and IE performed construction of GST fusion proteins, chimeric constructs, and liposome binding assays. AC, AA, and XG performed electrophysiological recordings in cell lines. JPG and XG participated in the design of the study and performed the statistical analysis. JPG and XG conceived the study, oversaw the research, and prepared the manuscript with help from all others. All authors read and approved the final manuscript.

Funding Information Supported by grants from Ministerio de Economia y Competitividad and Instituto de Salud Carlos III of Spain FIS PI14/00141 (XG) and FIS PI17/00296 (XG), RETICs Oftared RD12/0034/0003 (XG) and RD16/0008/0014 (XG), and Generalitat de Catalunya 2014SGR1165 (XG) and 2017SGR737 (XG). J.P.G. was supported by a Ramón y Cajal Research Contract (Ministerio de Economia y Competitividad RYC-2011-08589).

Compliance with Ethical Standards

Conflict of Interest The authors declare no competing financial interests

References

1. Goldstein SAN, Bayliss DA, Kim D et al (2005) International Union of Pharmacology. LV. Nomenclature and molecular relationships of two-P potassium channels. Pharmacol Rev 57:527–540. https://doi.org/10.1124/pr.57.4.12
2. Doyle DA, Morais Cabral J, Pfuetzner RA et al (1998) The structure of the potassium channel: molecular basis of K+ conduction and selectivity. Science 280:69–77
3. Enyedi P, Czirják G (2010) Molecular background of leak K+ currents: two-pore domain potassium channels. Physiol Rev 90:559–605. https://doi.org/10.1152/physrev.00029.2009
4. Bandulik S, Tauber P, Lalli E et al (2015) Two-pore domain potassium channels in the adrenal cortex. Pflugers Arch 467:1027–1042. https://doi.org/10.1007/s00424-014-1628-6
5. Duprat F, Lauritzen I, Patel A, Honoré E (2007) The TASK background K2P channels: chemo- and nutrient sensors. Trends Neurosci 30:573–580. https://doi.org/10.1016/j.tins.2007.08.003
6. Mathie A, Veale EL (2015) Two-pore domain potassium channels: potential therapeutic targets for the treatment of pain. Pflugers Arch 467:931–943. https://doi.org/10.1007/s00424-014-1655-3
7. Steinberg EA, Wafford KA, Brickley SG et al (2014) The role of K2P channels in anaesthesia and sleep. Pflugers Arch 467:907–916. https://doi.org/10.1007/s00424-014-1654-4
8. Sano Y, Inamura K, Miyake A et al (2003) A novel two-pore domain K+ channel, TRESK, is localized in the spinal cord. J Biol Chem 278:27406–27412
9. Bautista DM, Sigal YM, Milstein AD et al (2008) Pungent agents from Szechuan peppers excite sensory neurons by inhibiting two-pore potassium channels. Nat Neurosci 11:772–779. https://doi.org/10.1038/nn.2143
10. Tulleuda A, Cokic B, Callejo G et al (2011) TRESK channel contribution to nociceptive sensory neurons excitability: modulation by nerve injury. Mol Pain 7:30. https://doi.org/10.1186/1744-8069-7-30
11. Dobler T, Springauf A, Tovornik S et al (2007) TRESK two-pore-domain K+ channels constitute a significant component of background potassium currents in murine dorsal root ganglion neurones. J Physiol Lond 585:867–879. https://doi.org/10.1113/jphysiol.2007.145649
12. Usoskin D, Furlan A, Islam S et al (2015) Unbiased classification of sensory neuron types by large-scale single-cell RNA sequencing. Nat Neurosci 18:145–153. https://doi.org/10.1038/nn.3881
13. Chiu IM, Barrett LB, Williams EK et al (2014) Transcriptional profiling at whole population and single cell levels reveals somatosensory neuron molecular diversity. Elife. https://doi.org/10.7554/eLife.04660
14. Manteniotis S, Lehmann R, Flegel C et al (2013) Comprehensive RNA-Seq expression analysis of sensory ganglia with a focus on ion channels and GPCRs in trigeminal ganglia. PLoS One 8:e79523. https://doi.org/10.1371/journal.pone.0079523
15. Kang D, Kim D (2006) TREK-2 (K2P10.1) and TRESK (K2P18.1) are major background K+ channels in dorsal root ganglion neurons. Am J Physiol, Cell Physiol 291:C138–C146. https://doi.org/10.1152/ajpcell.00629.2005
16. Lennertz RC, Tsunozaki M, Bautista DM, Stucky CL (2010) Physiological basis of tingling paresthesia evoked by hydroxy-sanshool. J Neurosci 30:4353–4361. https://doi.org/10.1523/JNEUROSCI.4666-09.2010
17. Castellanos A, Andres A, Bernal L et al (2018) Pyrethroids inhibit K2P channels and activate sensory neurons. Pain 159:92–105. https://doi.org/10.1097/j.pain.0000000000001068
18. Lafrenière RG, Cader MZ, Poulin J-F et al (2010) A dominant-negative mutation in the TRESK potassium channel is linked to familial migraine with aura. Nat Med 16:1157–1160. https://doi.org/10.1038/nm.2216
19. Liu P, Xiao Z, Ren F et al (2013) Functional analysis of a migraine-associated TRESK K+ channel mutation. J Neurosci 33:12810–12824. https://doi.org/10.1523/JNEUROSCI.1237-13.2013
20. Zhou J, Chen H, Yang C et al (2017) Reversal of TRESK down-regulation alleviates neuropathic pain by inhibiting activation of gliocytes in the spinal cord. Neurochem Res 42:1288–1298. https://doi.org/10.1007/s11064-016-2170-z
21. Callejo G, Giblin JP, Gasull X (2013) Modulation of TRESK background K+ channel by membrane stretch. PLoS One 8:e64471. https://doi.org/10.1371/journal.pone.0064471
22. Guo Z, Cao Y-Q (2014) Over-expression of TRESK K(+) channels reduces the excitability of trigeminal ganglion nociceptors. PLoS One 9:e87029. https://doi.org/10.1371/journal.pone.0087029
23. Zhou J, Yang C-X, Zhong J-Y, Wang H-B (2013) Intrathecal TRESK gene recombinant adenovirus attenuates spared nerve injury-induced neuropathic pain in rats. Neuroreport 24:131–136. https://doi.org/10.1097/WNR.0b013e32835d8431
24. Zhou J, Yao S-L, Yang C-X et al (2012) TRESK gene recombinant adenovirus vector inhibits capsaicin-mediated substance P release from cultured rat dorsal root ganglion neurons. Mol Med Report 5:1049–1052. https://doi.org/10.3892/mmr.2012.778

25. Liu C, Au JD, Zou HL et al (2004) Potent activation of the human tandem pore domain K channel TRESK with clinical concentrations of volatile anesthetics. Anesth Analg 99:1715–1722, table of contents. https://doi.org/10.1213/01.ANE.0000136849.07384.44
26. Sonner JM, Cantor RS (2013) Molecular mechanisms of drug action: an emerging view. Annu Rev Biophys 42:143–167. https://doi.org/10.1146/annurev-biophys-083012-130341
27. Czirják G, Tóth ZE, Enyedi P (2004) The two-pore domain K+ channel, TRESK, is activated by the cytoplasmic calcium signal through calcineurin. J Biol Chem 279:18550–18558. https://doi.org/10.1074/jbc.M312229200
28. Czirják G, Enyedi P (2006) Targeting of calcineurin to an NFAT-like docking site is required for the calcium-dependent activation of the background K+ channel, TRESK. J Biol Chem 281:14677–14682. https://doi.org/10.1074/jbc.M602495200
29. Kang D, Kim G-T, Kim E-J et al (2008) Lamotrigine inhibits TRESK regulated by G-protein coupled receptor agonists. Biochem Biophys Res Commun 367:609–615. https://doi.org/10.1016/j.bbrc.2008.01.008
30. Kollert S, Dombert B, Döring F, Wischmeyer E (2015) Activation of TRESK channels by the inflammatory mediator lysophosphatidic acid balances nociceptive signalling. Sci Rep 5:12548. https://doi.org/10.1038/srep12548
31. Hughes S, Marsh SJ, Tinker A, Brown DA (2007) PIP2-dependent inhibition of M-type (Kv7.2/7.3) potassium channels: direct on-line assessment of PIP2 depletion by Gq-coupled receptors in single living neurons. Pflugers Arch 455:115–124. https://doi.org/10.1007/s00424-007-0259-6
32. Li Y, Gamper N, Hilgemann DW, Shapiro MS (2005) Regulation of Kv7 (KCNQ) K+ channel open probability by phosphatidylinositol 4,5-bisphosphate. J Neurosci 25:9825–9835. https://doi.org/10.1523/JNEUROSCI.2597-05.2005
33. Willars GB, Nahorski SR, Challiss RA (1998) Differential regulation of muscarinic acetylcholine receptor-sensitive polyphosphoinositide pools and consequences for signaling in human neuroblastoma cells. J Biol Chem 273:5037–5046
34. Allen V, Swigart P, Cheung R et al (1997) Regulation of inositol lipid-specific phospholipase cdelta by changes in Ca2+ ion concentrations. Biochem J 327(Pt 2):545–552
35. Rohács T (2016) Phosphoinositide signaling in somatosensory neurons. Advances in Biological Regulation 61:2–16. https://doi.org/10.1016/j.jbior.2015.11.012
36. Hilgemann DW, Feng S, Nasuhoglu C (2001) The complex and intriguing lives of PIP2 with ion channels and transporters. Sci STKE 2001:re19. https://doi.org/10.1126/stke.2001.111.re19
37. Chemin J, Patel AJ, Duprat F et al (2005) A phospholipid sensor controls mechanogating of the K+ channel TREK-1. EMBO J 24:44–53. https://doi.org/10.1038/sj.emboj.7600494
38. Chemin J, Patel AJ, Duprat F et al (2007) Up- and down-regulation of the mechano-gated K(2P) channel TREK-1 by PIP (2) and other membrane phospholipids. Pflugers Arch 455:97–103. https://doi.org/10.1007/s00424-007-0250-2
39. Lopes CMB, Rohács T, Czirják G et al (2005) PIP2 hydrolysis underlies agonist-induced inhibition and regulates voltage gating of two-pore domain K+ channels. J Physiol Lond 564:117–129. https://doi.org/10.1113/jphysiol.2004.081935
40. Brzeska H, Guag J, Remmert K et al (2010) An experimentally based computer search identifies unstructured membrane-binding sites in proteins. J Biol Chem 285:5738–5747. https://doi.org/10.1074/jbc.M109.066910
41. Letunic I, Doerks T, Bork P (2014) SMART: recent updates, new developments and status in 2015. Nucleic Acids Res 43:D257–D260. https://doi.org/10.1093/nar/gku949
42. Schultz J, Milpetz F, Bork P, Ponting CP (1998) SMART, a simple modular architecture research tool: identification of signaling domains. Proc Natl Acad Sci U S A 95:5857–5864
43. Callejo G, Castellanos A, Castany M et al (2015) Acid-sensing ion channels detect moderate acidifications to induce ocular pain. Pain 156:483–495. https://doi.org/10.1097/01.j.pain.0000460335.49525.17
44. Lemmon MA (2008) Membrane recognition by phospholipid-binding domains. Nat Rev Mol Cell Biol 9:99–111. https://doi.org/10.1038/nrm2328
45. Hernandez CC, Zaika O, Shapiro MS (2008) A carboxy-terminal inter-helix linker as the site of phosphatidylinositol 4,5-bisphosphate action on Kv7 (M-type) K +channels. J Gen Physiol 132:361–381. https://doi.org/10.1085/jgp.200810007
46. Shyng SL, Cukras CA, Harwood J, Nichols CG (2000) Structural determinants of PIP(2) regulation of inward rectifier K(ATP) channels. J Gen Physiol 116:599–608
47. Zeng W-Z, Liou H-H, Krishna UM et al (2002) Structural determinants and specificities for ROMK1-phosphoinositide interaction. American Journal of Physiology- Renal Physiology 282:F826–F834. https://doi.org/10.1152/ajprenal.00300.2001
48. Zhang H, He C, Yan X et al (1999) Activation of inwardly rectifying K+ channels by distinct PtdIns(4,5)P2 interactions. Nat Cell Biol 1:183–188. https://doi.org/10.1038/11103
49. Folch J (1942) Brain cephalin, a mixture of phosphatides. Separation from it of phosphatidylserine, phosphatidylenthanolamine, and a fraction containing an inositol phosphatide. J Biol Chem 146:35–44
50. Kimelberg HK, Papahadjopoulos D (1971) Interactions of basic proteins with phospholipid membranes. Binding and changes in the sodium permeability of phosphatidylserine vesicles. J Biol Chem 246:1142–1148
51. Fan Z, Makielski JC (1997) Anionic phospholipids activate ATP-sensitive potassium channels. J Biol Chem 272:5388–5395
52. Huang CL, Feng S, Hilgemann DW (1998) Direct activation of inward rectifier potassium channels by PIP2 and its stabilization by Gbetagamma. Nature 391:803–806. https://doi.org/10.1038/35882
53. Lopes CMB, Zhang H, Rohács T et al (2002) Alterations in conserved Kir channel-PIP2 interactions underlie channelopathies. Neuron 34:933–944
54. Veldhuis NA, Poole DP, Grace M et al (2015) The G protein-coupled receptor-transient receptor potential channel axis: molecular insights for targeting disorders of sensation and inflammation. Pharmacol Rev 67:36–73. https://doi.org/10.1124/pr.114.009555
55. Sandoz G, Bell SC, Isacoff EY (2011) Optical probing of a dynamic membrane interaction that regulates the TREK1 channel. Proc Natl Acad Sci U S A 108:2605–2610. https://doi.org/10.1073/pnas.1015788108
56. Rayaprolu V, Royal P, Stengel K et al (2018) Dimerization of the voltage-sensing phosphatase controls its voltage-sensing and catalytic activity. J Gen Physiol 150:683–696. https://doi.org/10.1085/jgp.201812064
57. Stauffer TP, Ahn S, Meyer T (1998) Receptor-induced transient reduction in plasma membrane PtdIns(4,5)P2 concentration monitored in living cells. Curr Biol 8:343–346
58. Falkenburger BH, Jensen JB, Dickson EJ et al (2010) Phosphoinositides: lipid regulators of membrane proteins. J Physiol Lond 588:3179–3185. https://doi.org/10.1113/jphysiol.2010.192153
59. Gamper N, Shapiro MS (2007) Regulation of ion transport proteins by membrane phosphoinositides. Nat Rev Neurosci 8:921–934. https://doi.org/10.1038/nrn2257
60. Braun G, Nemcsics B, Enyedi P, Czirják G (2011) TRESK background K(+) channel is inhibited by PAR-1/MARK microtubule affinity-regulating kinases in Xenopus oocytes. PLoS One 6:e28119. https://doi.org/10.1371/journal.pone.0028119
61. Chemin J, Girard C, Duprat F et al (2003) Mechanisms underlying excitatory effects of group I metabotropic glutamate receptors via

inhibition of 2P domain K+ channels. EMBO J 22:5403–5411. https://doi.org/10.1093/emboj/cdg528
62. Lesage F, Terrenoire C, Romey G, Lazdunski M (2000) Human TREK2, a 2P domain mechano-sensitive K+ channel with multiple regulations by polyunsaturated fatty acids, lysophospholipids, and Gs, Gi, and Gq protein-coupled receptors. J Biol Chem 275:28398–28405
63. Czirják G, Enyedi P (2010) TRESK background K(+) channel is inhibited by phosphorylation via two distinct pathways. J Biol Chem 285:14549–14557. https://doi.org/10.1074/jbc.M110.102020
64. Enyedi P, Veres I, Braun G, Czirják G (2014) Tubulin binds to the cytoplasmic loop of TRESK background K+ channel in vitro. PLoS One 9:e97854. https://doi.org/10.1371/journal.pone.0097854
65. Czirják G, Vuity D, Enyedi P (2008) Phosphorylation-dependent binding of 14-3-3 proteins controls TRESK regulation. J Biol Chem 283:15672–15680. https://doi.org/10.1074/jbc.M800712200
66. Hille B, Dickson EJ, Kruse M et al (2015) Phosphoinositides regulate ion channels. Biochimica et Biophysica Acta (BBA) - Molecular and Cell Biology of Lipids 1851:844–856. https://doi.org/10.1016/j.bbalip.2014.09.010
67. Maingret F, Patel AJ, Lesage F et al (2000) Lysophospholipids open the two-pore domain mechano-gated K(+) channels TREK-1 and TRAAK. J Biol Chem 275:10128–10133
68. Chemin J, Patel A, Duprat F et al (2005) Lysophosphatidic acid-operated K+ channels. J Biol Chem 280:4415–4421. https://doi.org/10.1074/jbc.M408246200
69. Comoglio Y, Levitz J, Kienzler MA et al (2014) Phospholipase D2 specifically regulates TREK potassium channels via direct interaction and local production of phosphatidic acid. Proc Natl Acad Sci U S A 201407160:13547–13552. https://doi.org/10.1073/pnas.1407160111
70. Basbaum AI, Bautista DM, Scherrer G, Julius D (2009) Cellular and molecular mechanisms of pain. Cell 139:267–284. https://doi.org/10.1016/j.cell.2009.09.028
71. Hucho T, Levine JD (2007) Signaling pathways in sensitization: toward a nociceptor cell biology. Neuron 55:365–376. https://doi.org/10.1016/j.neuron.2007.07.008
72. Keshavaprasad B, Liu C, Au JD et al (2005) Species-specific differences in response to anesthetics and other modulators by the K2P channel TRESK. Anesth Analg 101:1042–1049, table of contents. https://doi.org/10.1213/01.ane.0000168447.87557.5a
73. Czirják G, Enyedi P (2014) The LQLP Calcineurin-docking site is a major determinant of the calcium-dependent activation of human TRESK background K+ channel. J Biol Chem 289:29506–29518. https://doi.org/10.1074/jbc.M114.577684
74. Czirják G, Enyedi P (2006) Zinc and mercuric ions distinguish TRESK from the other two-pore-domain K+ channels. Mol Pharmacol 69:1024–1032. https://doi.org/10.1124/mol.105.018556
75. Marsh B, Acosta C, Djouhri L, Lawson SN (2012) Leak K^+ channel mRNAs in dorsal root ganglia: relation to inflammation and spontaneous pain behaviour. Mol Cell Neurosci 49:375–386. https://doi.org/10.1016/j.mcn.2012.01.002